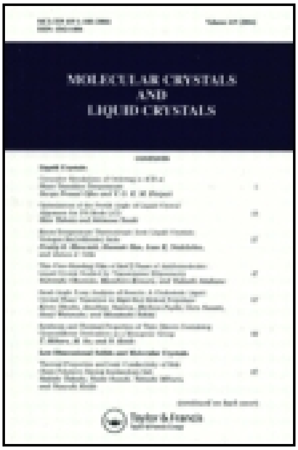

Molecular Crystals and Liquid Crystals

Publication details, including instructions for authors and subscription information:
http://www.tandfonline.com/loi/gmcl16

Disintegration Energy of Ferrocene Crystal in Triclinic Phase and Kinetic Study on Monotropic Transition from Monoclinic to Orthorhombic Phase

Megumi Naruse [a] [b] , Michio Sorai [a] & Minoru Sakiyama [a]

[a] Chemical Thermodynamics Laboratory, Faculty of Science, Osaka University, Toyonaka, Osaka, 560, Japan

[b] Hitachi Research Laboratory, Hitachi Ltd., Hitachi, Ibaraki, 319-12, Japan

To cite this article: Megumi Naruse , Michio Sorai & Minoru Sakiyama (1983): Disintegration Energy of Ferrocene Crystal in Triclinic Phase and Kinetic Study on Monotropic Transition from Monoclinic to Orthorhombic Phase, Molecular Crystals and Liquid Crystals, 101:3-4, 219-234

To link to this article: http://dx.doi.org/10.1080/01406568308072530

Mol. Cryst. Liq. Cryst., 1983, Vol. 101, pp. 219–234
0026-8941/83/1014-0219/$18.50/0

Printed in the United States of America

Disintegration Energy of Ferrocene Crystal in Triclinic Phase and Kinetic Study on Monotropic Transition from Monoclinic to Orthorhombic Phase†

MEGUMI NARUSE,‡ MICHIO SORAI and MINORU SAKIYAMA

Chemical Thermodynamics Laboratory, Faculty of Science, Osaka University, Toyonaka, Osaka 560, Japan

(*Received June 23, 1983*)

Cooling of single crystals of ferrocene below the λ-type phase transition at 163.9 K leads to crystal disintegration with explosive violence independently of the λ-type transition. The strain energy evolved at the disintegration ("the disintegration energy" for short) was determined to be (1.10 ± 0.11) kJ mol^{-1} by a drop calorimetry system using a low-temperature Calvet microcalorimeter. The disintegration energy was independent of the crystal size with four sieve fractions in the range 2.5–0.25 mm. The violent disintegration is interpreted here in terms of an energy transfer from the strain energy accumulated in the domain boundaries in a form of elastic energy to the kinetic energy of disintegrated crystallites. The speed of a crystallite with the grain size of 60–70 μm was estimated to be 110 m s^{-1}. On the other hand, kinetic aspect of a monotropic transition from the undercooled monoclinic to the stable orthorhombic phase at around 190 K has been investigated with the same drop calorimetry system. The monotropic transition was found to occur after a long induction period of 1–4 h. Kinetics of the transition can be well accounted for in terms of the Avrami theory. Growth of the stable phase proceeds three-dimensionally.

1. INTRODUCTION

Cooling of single crystals of ferrocene below the λ-type phase transition at 163.9 K invariably leads to crystal distortion.[1] Bodenheimer

---

†Contribution No. 62 from Chemical Thermodynamics Laboratory.

‡Present address: Hitachi Research Laboratory, Hitachi Ltd., Hitachi, Ibaraki 319-12, Japan.

and Low[2] examined this problem for single crystals grown from organic solvents by differential thermal analysis (DTA). Violent disintegration of the crystal with evolution of heat took place at a temperature in the range 125–108 K depending on the cooling rate, and hence they concluded that the λ-type phase transition and the disintegration of the crystal are independent phenomena. There exist, of course, many examples of crystals which are distorted or cracked at a phase transition temperature. This is often caused by a great difference in molar volume, crystal structure or molecular arrangement between adjacent phases. In the case of ferrocene, however, the volume change at the λ-point is extremely small and the molecular arrangements in both the adjacent phases resemble each other.[1,3-6] A remarkable difference between the disintegration of ferrocene crystal and the cracking phenomenon often encountered in usual crystals is that the former happens far below the transition point while the latter takes place at the same temperature as a phase transition. Moreover, the disintegration of ferrocene crystal occurs with explosive violence and with a large heat evolution.

Ogasahara *et al.*[7,8] reinvestigated the disintegration phenomenon for single crystals prepared by sublimation with techniques of DTA and adiabatic calorimetry. They determined the heat evolved at disintegration to be 0.61 kJ mol^{-1}. However, as they claimed, this value should be regarded as a lower limit of the heat evolution on account of their experimental limitations. We intended, therefore, to determine more accurately the strain energy evolved at crystal disintegration (designated hereafter as "the disintegration energy" for short) by a drop calorimetry system using a low-temperature Calvet microcalorimeter.

On the other hand, recent finding of a stable low-temperature (LT) phase of ferrocene crystal[7,8] disclosed a new aspect of the physicochemical properties of ferrocene. As reproduced in Figure 1 in terms of molar enthalpy,[7,8] the well-known λ-type phase transition at 163.9 K found by Edwards *et al.*[1] turned out to be a transition between metastable triclinic and monoclinic phases. The new LT-phase is transformed into the stable high-temperature (HT) monoclinic phase at 242 K.[7,8] The crystal structure of the stable LT-phase was soon proved to be orthorhombic.[9,10] Although the HT-phase is easily undercooled below 242 K, ferrocene crystals spontaneously undergo a monotropic transition into the stable LT-phase during a prolonged annealing around 190 K.[7-9] The rate of transition depends on crystal size and thermal history. Since detailed study on this monotropic transition has not been made, we aimed to elucidate its kinetic aspect

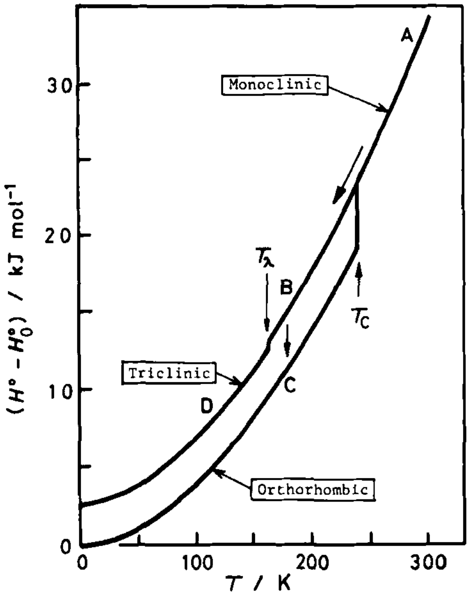

FIGURE 1 Enthalpy correlation diagram of ferrocene crystal.[7,8] The drop calorimetry experiment for the disintegration energy corresponds to a path A → D while the monotropic transition from the undercooled monoclinic to the stable orthorhombic phase occurs along a path B → C after a drop A → B.

by use of the present drop calorimetry system, which is specifically adequate for detection of such a slow thermal process.

2. EXPERIMENTAL

To examine the dependence of the disintegration energy on crystal size, sublimed crystals were screened through sieves with mesh-sizes of 1.30, 0.84, 0.35 and 0.25 mm to obtain four kinds of sieve fractions; A(*ca.* 2.5–1.3 mm), B(1.3–0.84 mm), C(0.84–0.35 mm) and D(0.35–0.25 mm). For the experiment aiming at the monotropic transition, only the sieve fraction A was used.

The design and performance of the present drop calorimetry system using a low-temperature Calvet microcalorimeter (Setaram Co., France) has been described in detail[11] and will be reported elsewhere.[12] The calorimeter is a twin-type conduction calorimeter, in which heat flux between a thermal sensing portion at the lowest part of each calorimetric well and the calorimeter heat sink is detected with a thermopile composed of several hundred thermocouples. The sensitivity is about

50 μV mW^{-1} over the whole working range (80 to 473 K). Two ampoules, one of which usually contains a sample, were allowed to equilibrate in a metal-block thermostat located above the calorimeter for 90 min, after which they were dropped freely into receivers housed in the wells of the calorimeter controlled at a constant temperature. The drop calorimetric system was calibrated by using an internal heater attached at the lowest part of the sample-side receiver. The accuracy and precision of the present calorimetry system have been proved to be satisfactory by use of heat capacity standard α-alumina (U.S. National Bureau of Standards, SRM-720).[11,12]

Since the sensitivities of the two calorimetric wells are slightly different, a drop of two empty ampoules brings about a small output signal even if their weights are equal. Therefore, a "blank test" without sample is inevitable prior to the proper experiments with sample. As schematically shown in Figure 2, an apparent enthalpy difference $\Delta H(\text{blank})$ was evaluated from the areas S_{B} and S_{C1} under the curves of the blank test (Figure 2a) and the first calibration (Figure 2b), respectively, and the electric work W_{1}^{el} supplied for calibration:

$$\Delta H(\text{blank}) = -W_{1}^{\mathrm{el}}(S_{\mathrm{B}}/S_{\mathrm{C1}}) = -S_{\mathrm{B}}/K_{\mathrm{B}} \qquad \left(K_{\mathrm{B}} \equiv S_{\mathrm{C1}}/W_{1}^{\mathrm{el}}\right). \tag{1}$$

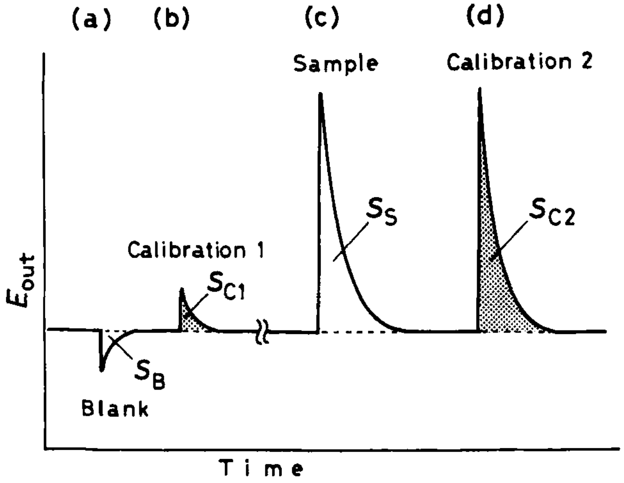

FIGURE 2 Schematic output curves for the drop calorimetry system using a low-temperature Calvet microcalorimeter. E_{out} is a differential electromotive force between thermopiles of the two calorimetric wells. Peaks (a), (b), (c) and (d) indicate curves of blank test, the first calibration, proper experiment and the second calibration, respectively.

To reduce the statistical errors involved in ΔH(blank), we repeated the blank test 6–8 times.

In the case of proper experiments, one ampoule contains ferrocene crystals while the other is empty. When two ampoules are dropped from the thermostat into the receiver of the calorimeter maintained at a lower temperature, a large peak is recorded. An apparent enthalpy difference ΔH(exp) was likewise determined from the areas S_S and S_{C2} under the curves for an experiment with sample (Figure 2c) and for the second calibration (Figure 2d), respectively, and the electric work W_2^{el} for calibration:

$$\Delta H(\exp) = -W_2^{el}(S_S/S_{C2}) = -S_S/K_S \qquad (K_S \equiv S_{C2}/W_2^{el}). \quad (2)$$

When the temperatures of the upper thermostat and the calorimeter heat sink are T_1 and T_2, respectively, the molar enthalpy difference of a sample ΔH_m between these temperatures can be related with the quantities given by Eqs. (1) and (2):

$$\begin{aligned}\Delta H_m &= H_m(T_2) - H_m(T_1)\\ &= (M/m)[\Delta H(\exp) - \Delta H(\text{blank})], \end{aligned} \quad (3)$$

where M and m are molar mass and mass of sample, respectively. The quantities obtained by a series of experiments were reduced to the enthalpy difference between common temperatures $T_1°$ and $T_2°$. Eq. (3) may then be written in the form,

$$\begin{aligned}\Delta H_m &= H_m(T_2°) - H_m(T_1°)\\ &= (M/m)[\Delta H(\exp) - \Delta H(\text{blank})] + \delta H_1 + \delta H_2, \end{aligned} \quad (4)$$

where δH_1 and δH_2 are the corrections due to slight deviation of experimental temperatures from $T_1°$ and $T_2°$, respectively:

$$\begin{aligned}\delta H_1 &= H_m(T_1) - H_m(T_1°),\\ \delta H_2 &= H_m(T_2°) - H_m(T_2). \end{aligned} \quad (5)$$

They were estimated from the heat capacity data already reported.[8]

Uncertainties given in this paper are standard deviation of the mean of the experimental results.

3. DISINTEGRATION PHENOMENON

The lowest temperature of disintegration of ferrocene crystals hitherto reported is 108 K[2] or higher,[8] hence the temperature of the heat sink T_2 was set at around 105 K while that of the upper thermostat T_1 was controlled at around 298 K. As the ampoule drops instantaneously, the cooling rate is extremely high and thus the monoclinic ferrocene is easily undercooled and transformed into the triclinic phase, along the path A → B → D in the enthalpy diagram shown in Figure 1.

A listing of the experimental data is given in Table I. Since matching of the sample-side ampoule with its receiver became increasingly poor during the series 1 experiments, it was interchanged with the reference-side ampoule in series 2. Thereby, ΔH(blank) was altered from 22.334 to 12.554 J. For samples A1 and D1, the crystals completely disintegrated into shatters by a first drop. For A4 and C1, however, a second drop experiment was necessary for complete disintegration. In the case of B2, the sensitivity of the second and third drop experiments slightly changed on account of different air-conditioning in the laboratory, by which $|\Delta H_{\mathrm{m}}|$ for these runs became rather large in comparison with those for other samples. Therefore, we assumed that the crystals of sample B2 might be completely disintegrated by the first and second drops as were other samples, and that the ΔH_{m} for the third drop should be replaced by the average value of ΔH_{m}(last drop) for B1, A4, D1 and C1. Validity of these assumptions is obvious if we compare the corrected $\Delta H_{\mathrm{m}}(= -25.651\ \mathrm{kJ\ mol^{-1}})$ for the third drop with $-25.649\ \mathrm{kJ\ mol^{-1}}$ for the fourth drop that was correctly executed. In Table I, the sample B1 is indicated as if the crystals were completely disintegrated by the first drop. As a matter of fact, however, the sample-side ampoule dropped several times in between the first and second drop experiments owing to operational miss. Absence of the first drop data for the samples A2 and A3 is likewise due to the operational miss.

The shattered crystallites had grain size of 60–70 μm or less independently of the sieve fractions of the untreated samples.

Prior to an estimation of the disintegration energy, we discuss here briefly the accuracy of the present experiment by comparing the ΔH_{m} for powdered crystals with the literature value derived from heat capacity data.[8] Table II lists the molar enthalpy difference between 104.83 and 297.35 K obtained from the last drop experiment of each sample in series 2. As described above, the last drop corresponds to a measurement for fine powdered crystals which have grain size of 60–70 μm or less and disintegrate no more. Therefore, these values do not include any contribution of the disintegration energy. The average value of the present experiment amounts to $\Delta H_{\mathrm{m}}(\mathrm{exp}) = (-25.65 \pm 0.07)\ \mathrm{kJ\ mol^{-1}}$ while the literature value[8] is $\Delta H_{\mathrm{m}}(\mathrm{cal}) = -25.58\ \mathrm{kJ\ mol^{-1}}$. Since they agree well with each other, the accuracy of the present calorimetry system is here also proved to be satisfactory.

TABLE I

Experimental data concerning the disintegration energy of ferrocene crystal

Sample[a]	Drop No. n	Mass m/g	$\frac{T_1}{\text{K}}$	$\frac{T_2}{\text{K}}$	$\frac{S}{\text{V s}}$	$\frac{K}{\text{V s J}^{-1}}$	$\frac{\Delta H(\text{exp})}{\text{J}}$	$\frac{\delta H_1}{\text{J mol}^{-1}}$	$\frac{\delta H_2}{\text{J mol}^{-1}}$	$\frac{\Delta H_m}{\text{kJ mol}^{-1}}$
Series 1 ($T_1° = 299.18$ K, $T_2° = 105.07$ K, ΔH(blank) = 22.334 J)										
A1	1	0.7044	299.23	105.04	3.28899	0.0404039	−81.403	9.5	2.3	−27.385
	2		299.03	105.03	3.12608	(0.0404039)[b]	−77.371	−28.4	3.0	−26.357
A2	2	0.7221	299.14	105.12	3.23114	0.0404067	−79.965	−7.6	−3.8	−26.367
A3	2	0.6746	299.26	105.04	2.96932	0.0404327	−73.439	15.1	2.3	−26.394
Series 2 ($T_1° = 297.35$ K, $T_2° = 104.83$ K, ΔH(blank) = 12.554 J)										
B1	1	0.7675	297.37	104.82	3.92048	0.0405188	−96.757	3.8	0.8	−26.491
	2		297.36	104.80	3.77476	0.0404730	−93.266	1.9	2.3	−25.646
A4	1	0.7361	297.29	104.84	3.72910	0.0405433	−91.978	−11.4	−0.8	−26.431
	2		297.31	104.80	3.64026	0.0405266	−89.824	−7.6	2.3	−25.879
	3		297.24	104.86	3.58350	0.0405303	−88.415	−20.8	−2.3	−25.541
D1	1	0.7401	297.20	104.84	3.82326	0.0405130	−94.371	−28.4	−0.8	−26.906
	2		297.21	104.84	3.63586	0.0405618	−89.638	−26.5	−0.8	−25.715
C1	1	0.7374	297.39	104.83	3.75000	0.0405283	−92.528	7.6	0.0	−26.503
	2		297.37	104.84	3.66955	0.0405650	−90.461	3.8	−0.8	−25.986
	3		297.33	104.84	3.62073	(0.0405330)[c]	−89.328	−3.8	−0.8	−25.706
B2	1	0.7368	297.11	104.91	3.72827	(0.0405330)[c]	−91.981	−45.4	−6.1	−26.446
	2		297.17	105.03	3.68440	0.0406019	−90.744	−34.1	−15.2	−26.131 (−25.814)[e]
	3		297.13	105.03	3.65700	(0.0406019)[b]	−90.070	−41.6	−15.2	−25.968 (−25.651)[d]
	4		297.08	105.01	3.59818	(0.0405330)[c]	−88.772	−51.1	−13.7	−25.649

[a] Grain size: A(2.5–1.3 mm), B(1.3–0.84 mm), C(0.84–0.35 mm) and D(0.35–0.25 mm).

[b] Adopting the value of the previous run.

[c] An average value of series 2.

[d] An average value of ΔH_m(last n) for B1, A4, D1 and C1.

[e] A value shifted according to (d).

TABLE II

Enthalpy difference of powdered ferrocene between 104.83 and 297.35 K

Sample	Drop No.	$\Delta H_m(\text{exp})$ / kJ mol^{-1}
Series 2		
($T_1° = 297.35$ K, $T_2° = 104.83$ K)		
A4	3	−25.541
B1	2	−25.646
B2	4	−25.649
C1	3	−25.706
D1	2	−25.715
$\Delta H_m(\text{exp}) = (-25.65 \pm 0.07)$ kJ mol^{-1}		
$\Delta H_m(\text{cal})^a = -25.58$ kJ mol^{-1}		

[a] Ref. 8.

The necessary data concerning estimation of the disintegration energy are summarized in Table III. The quantity $\Delta H_D(n)$ simply means an enthalpy difference between the last drop and the nth drop experiment:

$$\Delta H_D(n) = \Delta H_m(\text{last drop}) - \Delta H_m(n). \tag{6}$$

Total disintegration energy ΔH_D is then a sum of $\Delta H_D(n)$:

$$\Delta H_D = \sum_{n=1} \Delta H_D(n). \tag{7}$$

As far as the present grain sizes (2.5–0.25 mm) are concerned, we cannot discriminate among the disintegration energies of crystals with different sizes. The average value of ΔH_D is evaluated to be (1.10 ± 0.11) kJ mol^{-1}, in which the value for B1 has not been included because of the reason described above. The disintegration energy of (1.10 ± 0.11) kJ mol^{-1} determined here is much higher than 0.61 kJ mol^{-1} obtained previously as a lower limit.[8] Quite interestingly, the present disintegration energy is significantly higher than the enthalpy of the λ-type transition (0.90 kJ mol^{-1}).[7,8] This fact coincides with the results of DTA.[8]

A question that immediately arises is in what temperature region the strain energy begins to be stored. It is true that large crystals do not have the strain energy above the λ-point because the stabilization enthalpy of large crystals from the undercooled monoclinic to the

TABLE III

Disintegration energy of ferrocene crystal

Sample	Drop No. n	$\Delta H_m(n)$ / kJ mol^{-1}	$\Delta H_D(n)$ / kJ mol^{-1}	ΔH_D / kJ mol^{-1}
		Series 1		
A1	1	-27.385	1.028	1.028
	2	-26.357		
		Series 2		
A4	1	-26.431	0.890	1.228
	2	-25.879	0.338	
	3	-25.541		
B1	1	-26.491	0.845	0.845[a]
	2	-25.646		
B2	1	-26.446	0.797	(0.964)[b]
	2	(-25.814)	(0.165)	
	3	(-25.651)	(0.002)	
	4	-25.649		
C1	1	-26.503	0.797	1.077
	2	-25.986	0.280	
	3	-25.706		
D1	1	-26.906	1.191	1.191
	2	-25.715		

$\Delta H_D{}^c = (1.10 \pm 0.11)$ kJ mol^{-1}

[a] Between drop experiments 1 and 2, the sample ampoule dropped several times.

[b] Based on the corrected ΔH_m.

[c] The value for B1 has not been included.

stable orthorhombic phase is identical with that of the disintegrated crystals[8] and also because Raman spectrum of a ferrocene single crystal is identical with that of a fragment of a disintegrated crystal.[13] As suggested previously,[2,8] the disintegration of ferrocene crystal and the λ-type phase transition are independent phenomena. Nevertheless, existence of the latter is a necessary condition for occurrence of the former. That is to say, the disintegration phenomenon occurs only in the triclinic phase below the λ-point. Therefore, it is very likely that the strain energy gradually begins to be stored in a crystal below the λ-point with decreasing temperature. When the strain energy exceeds a certain threshold value, the crystal suddenly disintegrates into fine powder with evolution of heat.

The next question is in what parts of a crystal such a large strain energy as 1.10 kJ mol^{-1} is stored and, moreover, a mystery is why the disintegration occurs with explosive violence. If the strain energy were stored in each ferrocene molecule as excess energy due to deformed potential curves of particular interatomic vibrations, the energy evolved at the disintegration would be rapidly consumed for excitation of these vibrations without accompanying drastic fracture of a crystal and, as the result, temperature of the specimen would be raised. This kind of phenomenon has been found for some glass-forming materials,[14] in which a sudden heat evolution with simultaneous luminescence and crack sound occurs near the glass transition region on cooling but the solid materials are never shattered into powder.

Bodenheimer and Low[2] assumed the existence of domains which finally disintegrate into single domain crystallites. If this is the case, the strain energy might be stored in the domain boundaries. This idea seems to be supported if we regard the situation as follows; the strain energy accumulated in the domain boundaries in a form of elastic energy might be in the first place transferred to the kinetic energy of disintegrated crystallites, which would then be transferred to the potential energy of ferrocene molecules by a collision among the flying crystallites. Let us regard the dimension of a crystallite as being a cube of 65 μm according to the fact that the grain size of the disintegrated crystals is 60–70 μm or less. The volume of a grain is then $v = 2.7 \times 10^{-7}\ \mathrm{cm}^3$. As the density[6] at, say, 148 K is $\rho = 1.57\ \mathrm{g\ cm}^{-3}$, the mass of a grain is $m = \rho v = 4.2 \times 10^{-7}$ g. The number of grains amounts to $n = M/m = 4.4 \times 10^8\ \mathrm{mol}^{-1}$, where $M(= 186.04)$ is the molar mass of ferrocene. Since the disintegration energy is $\Delta H_\mathrm{D} = 1.10$ kJ mol^{-1}, so its partition per grain is $\epsilon = \Delta H_\mathrm{D}/n = 25\ \mathrm{g\ cm}^2\ \mathrm{s}^{-2}$. If we equate it to the kinetic energy of a grain in the form,

$$\epsilon = \tfrac{1}{2}mV^2, \tag{8}$$

the speed of a flying crystallite can be estimated to be as high as $V = 110\ \mathrm{m\ s}^{-1}$. This high speed seems to be responsible for the disintegration phenomenon of ferrocene crystal with explosive violence.

Similar disintegration phenomenon was recently found for ferrocene-d_{10}.[15] We can also find a brief description concerning a disintegration of nickellocene below 163 K in the previous literature.[16] However, in view of the facts that there exists no λ-type phase transition in nickellocene at least below room temperature[17,18] and that its crystal structure is monoclinic,[19–21] the disintegration phenomenon of nickellocene[16] seems to be different in nature from that of ferrocene. When a large ferrocene crystal is stored for a long period in the undercooled monoclinic phase, many cracks really appear and the crystal becomes opaque, but it still keeps the same size as the original crystal.[8] In addition, this cracking phenomenon occurs as the result of the monotropic phase transition from the undercooled monoclinic to the stable orthorhombic phase. Even in this sense, the disintegration phenomena of nickellocene and ferrocene are different in nature.

Finally, it may be remarked that the violent disintegration of ferrocene occurs not only for crystals prepared by sublimation[1,8] and recrystallization[2] from organic solvents but also for crystals obtained from melt.

4. MONOTROPIC TRANSITION FROM MONOCLINIC TO ORTHORHOMBIC PHASE

We set the temperature of the heat sink T_2 at around 190 K, at which the monotropic transition from the undercooled monoclinic to the stable orthorhombic phase proceeds most effectively.[7,8] The specimen used here had a crystal size of 2.5–1.3 mm, and its mass was 0.7336 g. When two ampoules (one containing sample and the other being empty) are dropped from the thermostat at T_1 (near room temperature) to the calorimetric wells at T_2, a sharp peak of output signal is observed and then followed by a broad peak with intensity of the order of one hundredth as compared with the former one. The former corresponds to the enthalpy difference between T_2 and T_1 along the path A → B shown in Figure 1 while the latter results from the sluggish monotropic phase transition along the path B → C.

Freshly sublimed crystals were loaded into one of the ampoules and the first drop experiment was performed. As shown in Figure 3, a weak output signal due to the monotropic transition became gradually detectable after an induction period of 4 h. Its intensity increased with time to give a maximum and finally the signal ceased after 26 h. The transition enthalpy ΔH_{trs} was evaluated to be 3.49_6 kJ mol^{-1} from the area under this peak. This value was only 86% of the enthalpy difference determined by the heat capacity measurements.[7,8] This incompleteness of the monotropic transition is in accord with the previous finding[7,8] that a virgin specimen, not experiencing the metastable triclinic phase, is difficult to completely transform into the stable LT-phase. Therefore, we demounted the sample ampoule from the calorimeter and immersed it several times in liquid nitrogen. As the ferrocene crystals became already opaque during the first drop experiment, this drastic treatment did not lead to any disintegration of the crystals in the ampoule.

The second drop experiment was then executed for the specimen thus treated (see Figure 3). The induction period was shortened to 1 h after a drop. Moreover, the monotropic transition was completed in only 12 h, extremely short in comparison with the first drop experiment. These facts seem to be accounted for in terms of the formation of lattice defects in the crystals as follows: Once the crystals experience the triclinic phase below the λ-point, defects would be produced in the crystal lattice and they would become the activation points of nucleation for the appearance of the orthorhombic phase.

To confirm reproducibility of the monotropic transition, successive runs were made. The results are shown in Figure 4 and their numerical data are summarized in Table IV. Height of the transition peak became higher and the transition finished in a shorter period in progression from the second to the fourth drop experiment. This fact may be interpreted in terms of formation of a memory or easy path for molecular rearrangements by repeated thermal cycling between the monoclinic and the orthorhombic phases. In spite of the largest

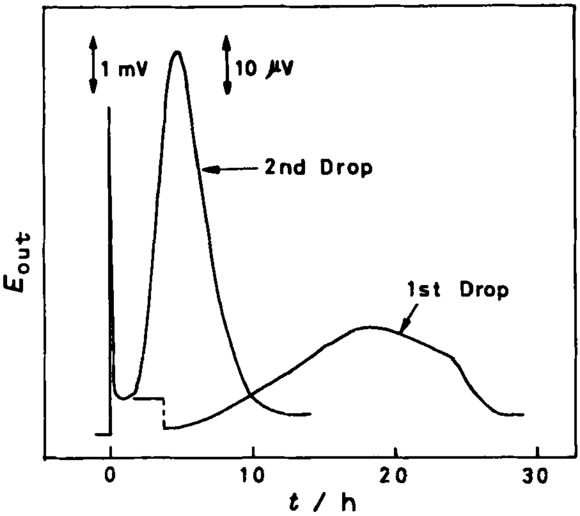

FIGURE 3 Drop calorimetric curves for the monotropic transition of ferrocene crystal. The first sharp peak corresponds to the enthalpy difference between the initial (T_1) and final (T_2) temperatures of the sample while the second broad peak results from the monotropic transition at T_2. Note that the sensitivity of output signal is increased by one hundred times in the latter as compared with the former.

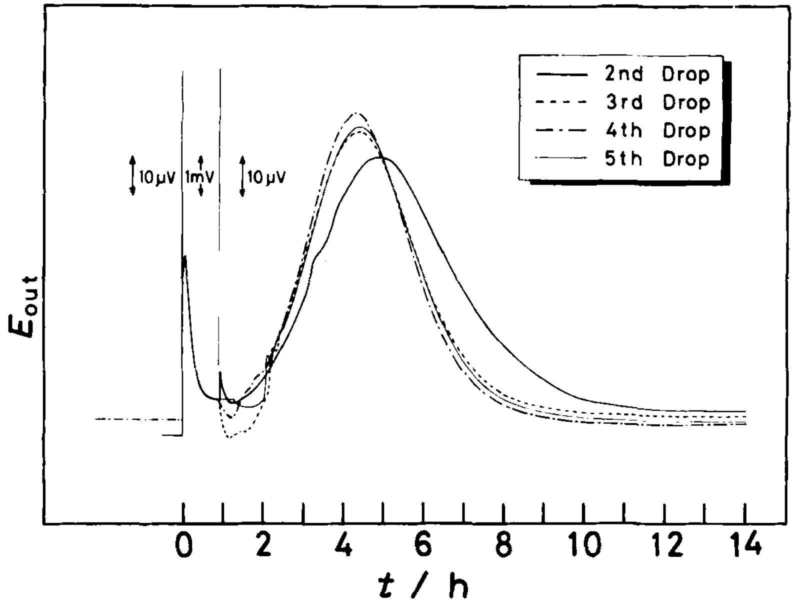

FIGURE 4 Drop calorimetric curves for the monotropic transition of ferrocene crystal (*cf.*, the caption of Figure 3).

TABLE IV

Monotropic phase transition from the undercooled monoclinic to the stable orthorhombic phase of ferrocene crystal

Experimental[a] No.	Standing period at T_1 / min	T_2 / K	ΔH(exp) / J	ΔH_{trs}(exp) / kJ mol^{-1}	ΔH_{trs}(cal)[b] / kJ mol^{-1}	Fraction of[c] stable phase α
1[d]	90	187.89	13.78	3.49_6	4.080	86
2	90	188.81			4.086	
3[d]	130	188.42	16.01	4.06_0	4.084	99
4	80	186.99	15.659	3.971	4.072	97.5
5	180	186.94	15.539	3.952	4.072	97.1

[a] Mass of sample = 0.7336 g. After the experiment of No. 1, the sample ampoule was immersed several times in liquid nitrogen.

[b] Ref. 8.

[c] $\alpha = 100 \times \Delta H_{trs}(\text{exp})/\Delta H_{trs}(\text{cal})$.

[d] Estimated graphically.

number of a drop, however, the transition in the fifth drop experiment proceeded more slowly than the fourth drop. This fact may be caused by a partly fading effect of the memory during a long standing period in the thermostat. The fraction of the stable phase was 99, 97.5 and 97.1% for the 3rd, 4th and 5th drop experiments, respectively. The fact that the transformation from the monoclinic to the orthorhombic phase takes much longer time for the remaining few per cent fraction is in accord with the previous finding.[7-9]

We analyzed the transition behavior within the framework of the Avrami theory[22-24] by taking the fourth drop experiment as an example. As is well-known, his theory has been developed with an assumption that the new phase is nucleated by germ nuclei which already exist in the original phase. This assumption seems to be satisfied in the case of ferrocene crystal because enough germ nuclei of the orthorhombic phase would be produced during the rather long induction period. According to his theory, the fraction of the stable phase at time t can be expressed in the form,

$$\alpha(t) = 1 - \exp(-Bt^k), \tag{9}$$

where B is a constant determining the transition rate and k is an index characterizing the growth of the stable phase: $k = 1$, 2 and 3 correspond to linear, plate-like and polyhedral growth, respectively.

The fraction of the orthorhombic phase, α, was estimated by integrating the peak area every thirty minutes. The results are plotted in Figure 5 against the time after a drop, in which a S-shaped curve typical of the Avrami theory is obtained. Eq. (9) can be rewritten in

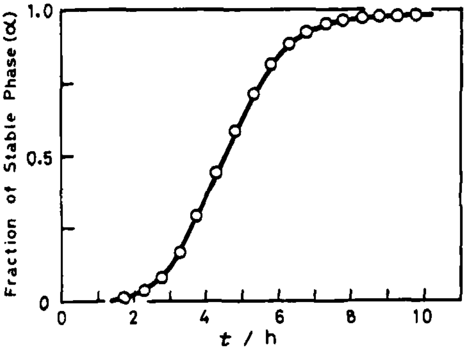

FIGURE 5 A plot of the fraction of the orthorhombic phase of ferrocene against the time after a drop for the fourth drop experiment at 186.99 K.

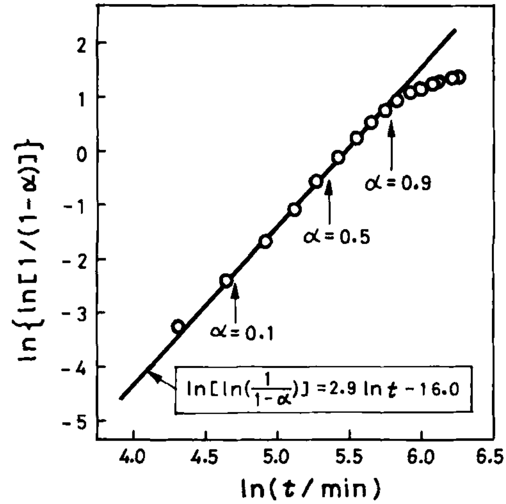

FIGURE 6 An Avrami's plot for the growth of the orthorhombic phase of ferrocene crystal in the monoclinic phase at 186.99 K. The origin of time is taken at 60 min after a drop because of the existence of an induction period.

the form,

$$\ln\{\ln[1/(1-\alpha(t))]\} = k \ln t + \ln B. \qquad (10)$$

Figure 6 represents a plot of $\ln\{\ln[1/(1-\alpha(t))]\}$ against $\ln t$, in which the time is counted from 60 min after a drop because of the existence of an induction period. The plot gives a straight line over a wide range of $0 < \alpha(t) < 0.9$. This fact obviously indicates that the present monotropic transition can be described by the Avrami theory. The slope of this straight line yielded $k = 2.9$. Although the parameter k somewhat depends on a choice of the origin of time, the value of $k = 2.9$ can essentially be regarded as being 3. Therefore, the growth of the orthorhombic phase of ferrocene crystal can be concluded to proceed three-dimensionally in the monoclinic phase.

Acknowledgment

The authors acknowledge Messrs. K. Ogasahara and Y. Shiomi for preparation of sieved crystals of ferrocene.

References

1. J. W. Edwards, G. L. Kington and R. Mason, *Trans. Faraday Soc.*, **56**, 660 (1960).
2. J. S. Bodenheimer and W. Low, *Phys. Lett.*, **36A**, 253 (1971).

3. G. Calvarin and J. F. Bérar, *J. Appl. Cryst.*, **8**, 380 (1975).
4. P. Seiler and J. D. Dunitz, *Acta Cryst.*, **B35**, 1068 (1979).
5. F. Takusagawa and T. F. Koetzle, *Acta Cryst.*, **B35**, 1074 (1979).
6. P. Seiler and J. D. Dunitz, *Acta Cryst.*, **B35**, 2020 (1979).
7. K. Ogasahara, M. Sorai and H. Suga, *Chem. Phys. Lett.*, **68**, 457 (1979).
8. K. Ogasahara, M. Sorai and H. Suga, *Mol. Cryst. Liq. Cryst.*, **71**, 189 (1981).
9. J. F. Bérar, G. Calvarin, D. Weigel, K. Chhor and C. Pommier, *J. Chem. Phys.*, **73**, 438 (1980).
10. P. Seiler and J. D. Dunitz, *Acta Cryst.*, **B38**, 1741 (1982).
11. M. Naruse, Thesis for master of science degree, Osaka University (1983).
12. M. Naruse and M. Sakiyama, to be published.
13. J. Bodenheimer, E. Loewenthal and W. Low, *Chem. Phys. Lett.*, **3**, 715 (1969).
14. K. Kishimoto, H. Suga and S. Seki, *J. Non-Cryst. Solids*, **13**, 357 (1973/74).
15. M. Sorai and Y. Shiomi, to be published in *Mol. Cryst. Liq. Cryst.*.
16. M. Nussbaum and J. Voitländer, *Z. Naturforsch.*, **20a**, 1417 (1965).
17. C. Azokpota, G. Calvarin and C. Pommier, *J. Chem. Thermodyn.*, **8**, 283 (1976).
18. I. B. Rabinovich, V. P. Nistratov, M. S. Sheiman and G. V. Burchalova, *J. Chem. Thermodyn.*, **10**, 523 (1978).
19. G. Calvarin and D. Weigel, *J. Appl. Cryst.*, **9**, 212 (1976).
20. P. Seiler and J. D. Dunitz, *Acta Cryst.*, **B36**, 2255 (1980).
21. G. Clec'h and G. Calvarin, *Mol. Cryst. Liq. Cryst.*, **75**, 345 (1981).
22. M. Avrami, *J. Chem. Phys.*, **7**, 1103 (1939).
23. M. Avrami, *J. Chem. Phys.*, **8**, 212 (1940).
24. M. Avrami, *J. Chem. Phys.*, **9**, 177 (1941).